Lecture 10 – PET

This lecture will cover: *(CH3.13-3.21)*

– Positron Emission Tomography (PET)

- Introduction of PET
- Radiotracer used for PET/CT
- Instrumentation of PET/CT
- PET imaging
- Data processing in PET/CT
- Image characteristics
- Time-of-flight PET

– Clinical applications of Nuclear Medicine

(*Supplementary reading: The Essential Physics of Medical Imaging CH19.3)*

Introduction

- Emission tomography for functional imaging of the body;
- 100-1000 times higher SNR and significantly better spatial resolution than SPECT;
- Based on positron emission reaction and pair production;
- The fundamental difference between SPECT and PET is the radiotracers.
- PET/CT has largely replaced stand-alone PET

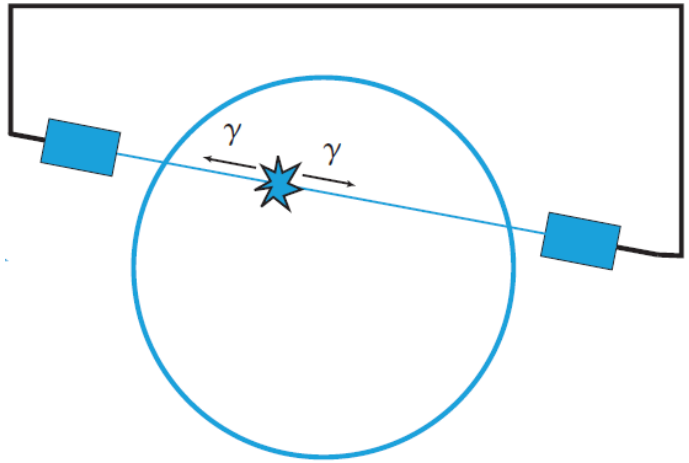

Fig. In PET, photon pairs are detected by electronic coincidence circuits connecting pairs of detectors..

Radiotracer used for PET/CT

- Undergo radioactive decay by emitting a positron

$$p^+ \rightarrow n + e^+ \qquad e^+ + e^- = 2\gamma$$

- Isotopes: ^{11}C, ^{15}O, ^{18}F, ^{13}N

Example : $^{18}_{9}F \rightarrow {}^{18}_{8}O + e^+ + n$ $\qquad$ $^{11}_{6}C \rightarrow {}^{11}_{5}B + e^+ + n$

Table. Properties and applications of the most common PET radiotracers

Radionuclide	Half-life (minutes)	Radiotracer	Clinical applications
^{18}F	109.7	^{18}FDG	oncology, inflammation, cardiac viability
^{11}C	20.4	^{11}C-palmitate	cardiac metabolism
^{15}O	2.07	$H_2{}^{15}O$	cerebral blood flow
^{13}N	9.96	$^{13}NH_3$	cardiac blood flow
^{82}Rb	1.27	$^{82}RbCl_2$	cardiac perfusion

Radiotracer used for PET/CT

- Radiotracers for PET are structural analogues (类似物) of biologically active molecules in which one or more of atoms have been replaced by a radioactive atom
- Most commonly used Isotopes is ^{18}F-fluorodeoxyglucose (FDG, ^{18}F 脱氧葡萄糖),

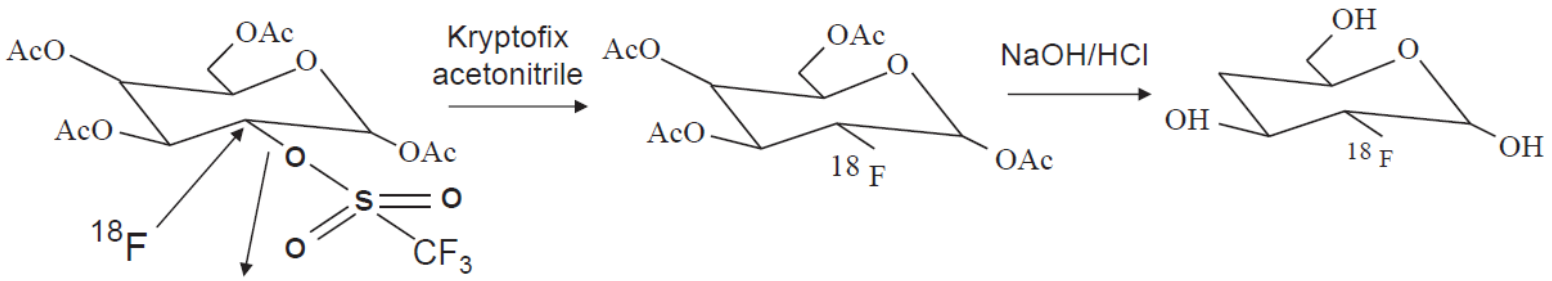

Figure 3.23

The most common synthesis of ^{18}FDG.

Radioactive transformation and coincidence

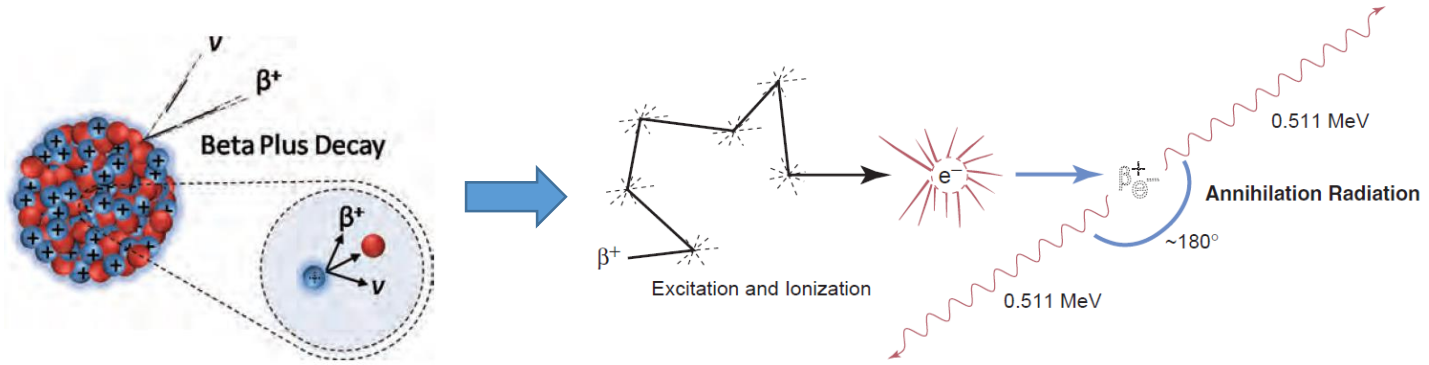

Fig 1. (Left) the positron decay; (Right) Annihilation radiation, forms an intrinsic LOR (line-of-reconstruction, or line-of-response).

Fig 2. True coincidence (left), scatter coincidence (center), and random (accidental) coincidence (right). A scatter coincidence is a true coincidence, because it is caused by a single nuclear transformation, but results in a count attributed to the wrong LOR (dashed line). The random coincidence is also attributed to the wrong LOR.

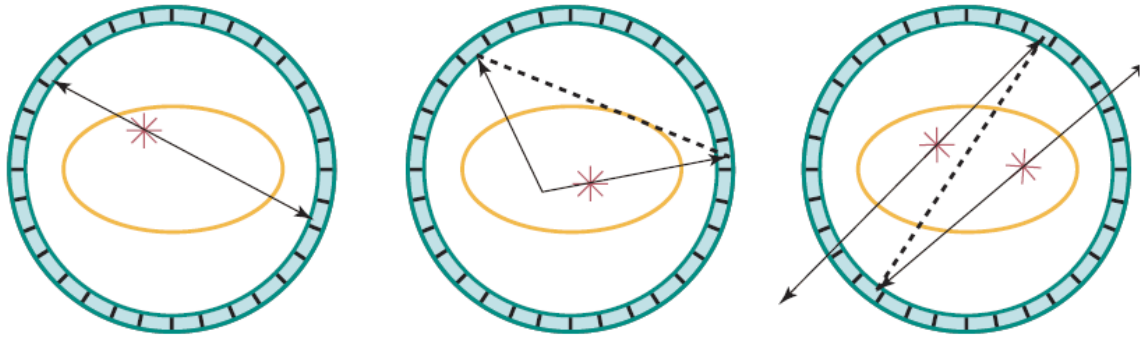

Instrumentations of PET

Higher SNR and spatial resolution comparing to SPECT due to:

- Collimation not being required;
- Reduced attenuation of higher energy γ-rays in tissue;
- The use of a complete ring of detector.

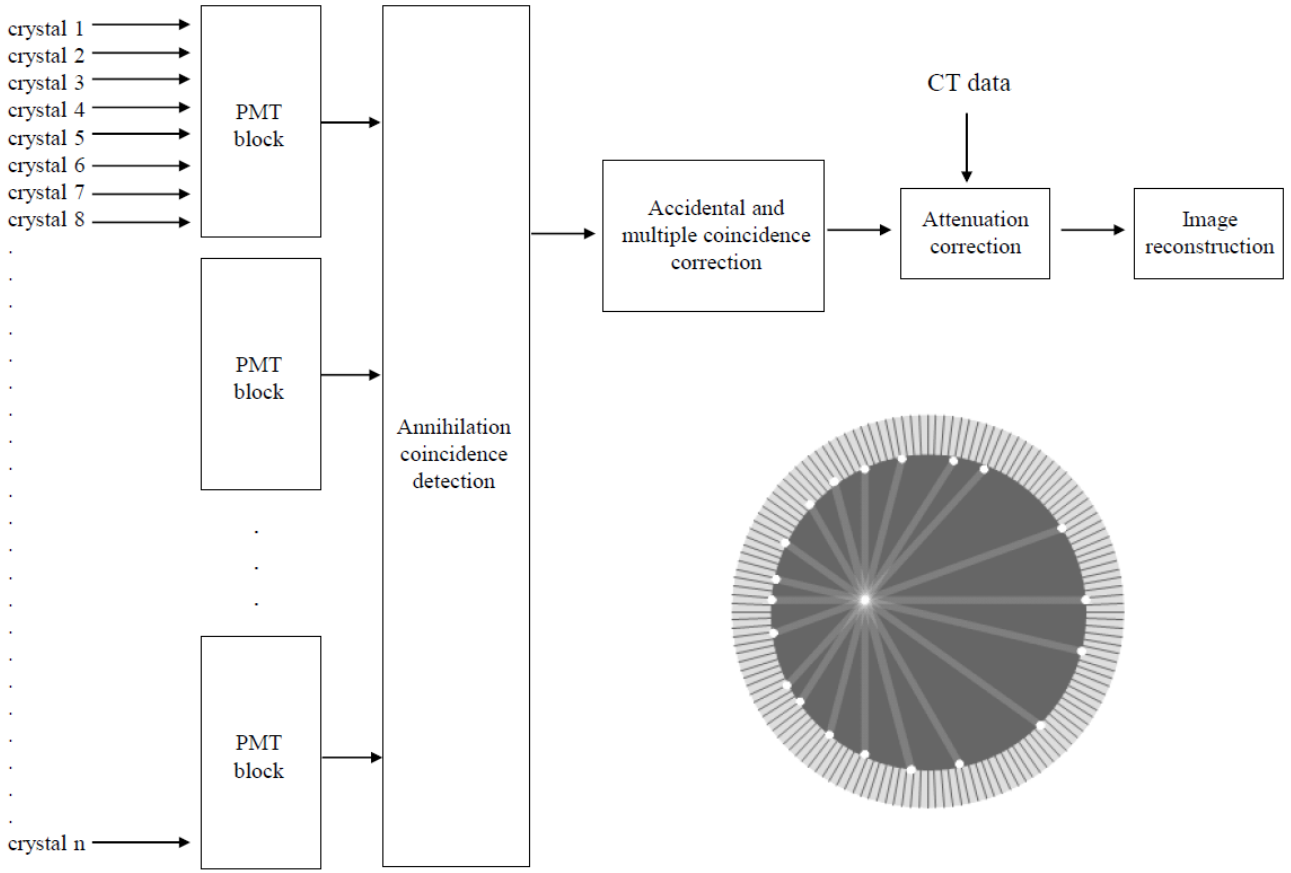

Fig. (top) The elements of a PET/CT system. (inset) Formation of lines-of-response in the PET detector ring.

Detectors for PET

The ideal detector crystal has:

- A high γ-ray detection efficiency ;
- A short decay time to allow a short coincidence resolving time;
- A high emission intensity to allow more crystals to be coupled to a single PMT;
- An emission wavelength near 400nm for maximum sensitivity for PMTs;
- Optical transparency at the emission wavelength;
- An index of refraction close to 1.5 to ensure efficient transmission of light between crystal and the PMT.

Properties of PET detectors

	Decay time (ns)	Emission intensity	Efficiency (ϵ^2)	$\lambda_{emitted}$ (nm)	η
BGO	300	0.15	0.72	480	2.15
LSO(Ce)	40	0.75	0.69	420	1.82
BaF_2	0.8_{prim}, 600_{sec}	0.12	0.34	220, 310	1.49
GSO(Ce)	60_{prim}, 600_{sec}	0.3	0.57	430	1.85
NaI(Tl)	230_{prim}, $10^4{}_{sec}$	1.0	0.24	410	1.85

GSO(Ce):cerium-doped gadolinium orthosilicate (Gd_2SiO_5),LSO(Ce): cerium-doped lutetium orthosilicate (Lu_2SiO_5). Both primary and secondary decay times are reported, efficiency values are for 2 cm thickness crystals and represent detection of both γ-rays striking the two detectors, η is the refractive index, and decay times are expressed as primary and secondary decays; the intensity is relative to a value of 1.0 for NaI(Tl).

Block detector

- A large block of BGO (dimension of 50*50*30mm) with a series of partial cuts through it on the top;
- The cuts is filled with light-reflecting material to prevent light from producing a very broad LSF when reach the bottom of crystal;
- Considered as separate detector array due to the partial cut.
- PMTs couple to Block and localize γ-ray using the same Anger principle as gamma camera.

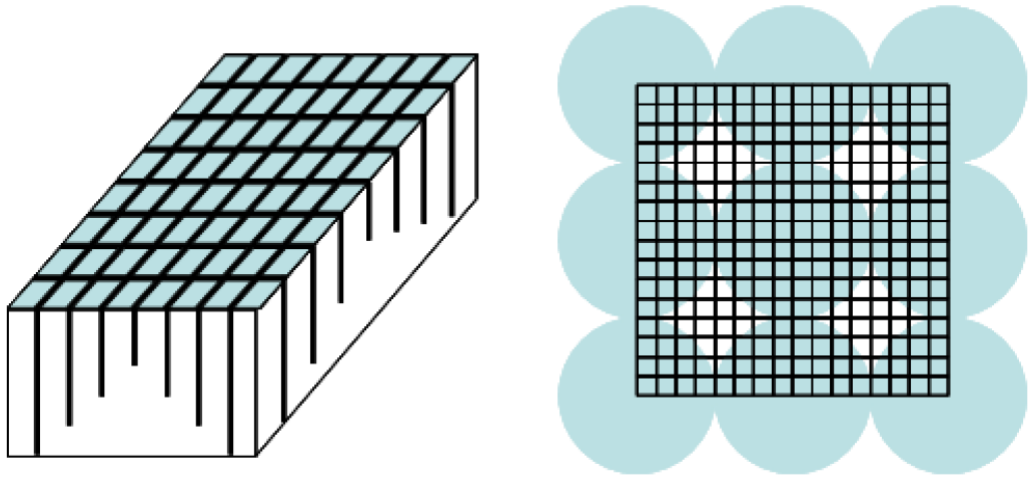

Fig. (left) A large BGO crystal cut into 64 effective separate elements. The partial cuts are filled with light-reflecting material. (right) Quadrant-sharing arrangement of the BGO crystals with PMTs shown by the circles..

PMT and PHA

- The operation of photomultiplier (PMT) and pulse height analyzer (PHA) is identical to the planar scintigraphy and SPECT.
- The voltage within pre-determined range generates a “logic pulse”, typically 6-10ns long
- The pulse is sent to the coincidence detector
- The energy resolution of BGO crystals is ~20%, therefore the energy window is 450-650keV

Annihilation coincidence detection

- Coincidence resolving time:
  - the time window that is allowed for a second γ-ray to be recorded and assigned to the same annihilation after the first γ-ray has been detected;
  - Typically value of 6-12ns
- In-coincidence detectors;
- True coincidence: two γ-rays strike the in-coincidence detectors in the coincidence resolving time.
- LOR (line of response, 响应线) can be established between the two detectors with striking γ-rays.

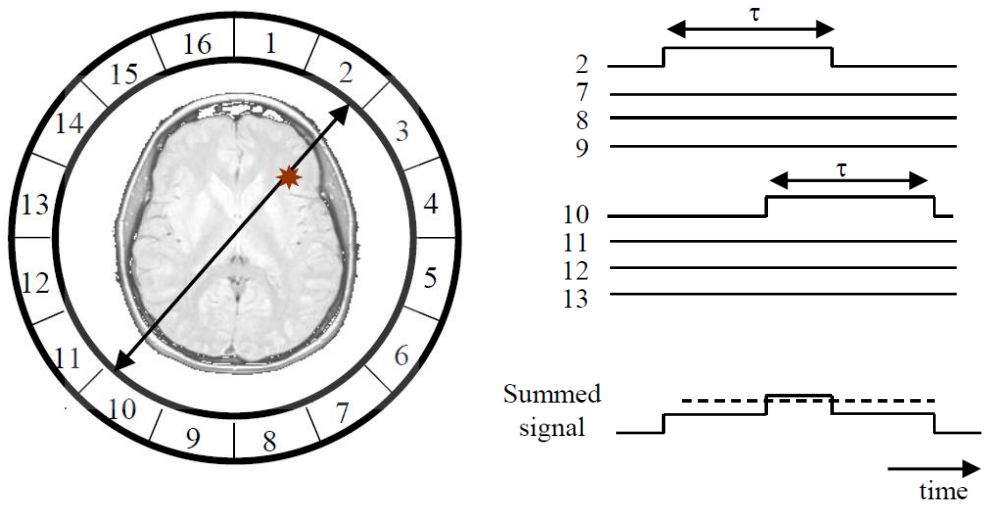

Fig. The principle of annihilation coincidence detection. (left) The two γ-rays reach detectors 2 and 10, triggering respective logic pulses of length τ. (right) If both logic pulses are sent to the coincidence detector within the system coincidence resolving time 2τ, then the summed signal lies above the threshold value (dashed line) and a coincidence is recorded.

2D & 3D PET Imaging

- Retractable lead collimation septa positioned between each rings
  - 2D mode: extended septa
  - 3D mode: retracted septa
- 2D mode
  - Reduce the amount of scattered γ-rays detected;
  - Produce uniform sensitivity profile along the axial dimension;
  - 2n-1 image planes: image plane can be formed between 2 crystals in the same ring (direct plane) or adjacent rings (cross planes)
- 3D mode
  - Higher sensitivity by about factor of 10
  - Higher SNR and reduced scan time
  - More random and scattered coincidence
  - Sensitivity is higher in the center than two ends

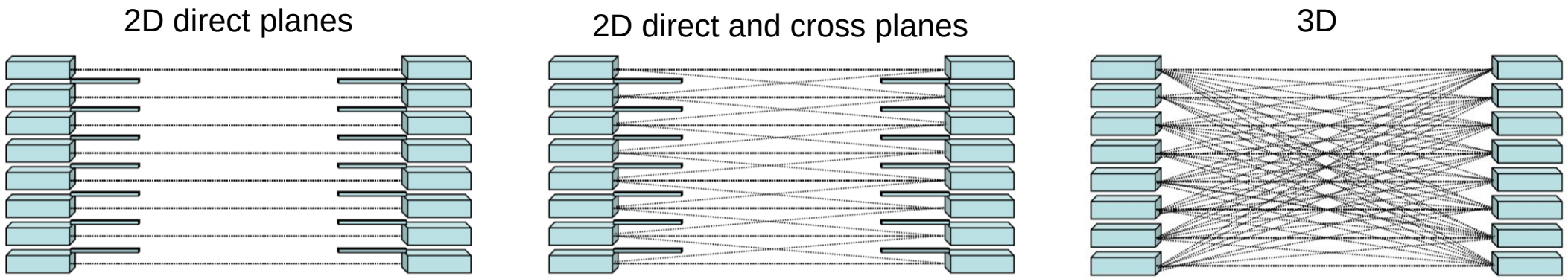

Fig. Three different data acquisition modes used for PET scans. Note that the septal collimators are retracted for 3D mode

Data processing in PET/CT

- **Attenuation correction**
  - Using PET/CT scanner for estimation of attenuation coefficients and anatomical structures.
  - Standard attenuation coefficient value assigned at 511keV
- **Correction for accidental and multiple coincidence**
- **Correction for scattered coincidence**
- **Correction for dead time:** The three major sources of dead time in PET
  - The time taken to integrate the charge for the PMTs
  - The processing of a coincidence event
  - The presence of multiple coincidences in which the data are discarded

Correction for accidental and multiple coincidence

- Accidental (random) coincidence
  - ~20% for head scan and 50% for body scan;
  - Uniformly distribution across imaging FOV
- Methods of correction
  - Additional parallel timing circuitry
    - ✓ The second coincidence timing window starts significantly later (typically 60ns) after an event is recorded
    - ✓ The accidental coincidences are subtracted
  - Uniformly distribution across imaging FOV
    - ✓ The rate of recorded accidental coincidence : $C_{ij}^{acc} = 2\tau R_i R_j$, where R_i and R_j are the single count rates in the individual detectors **i** and **j**, and 2τ is the coincidence resolving time;
    - ✓ Multiple coincidence: $M_{ij} \approx C_{ij}^{acc} \tau R_{ij} N_{ij}$, where N_{ij} is the total number of detectors operating in coincidence with either of the two detector **i** and **j**.

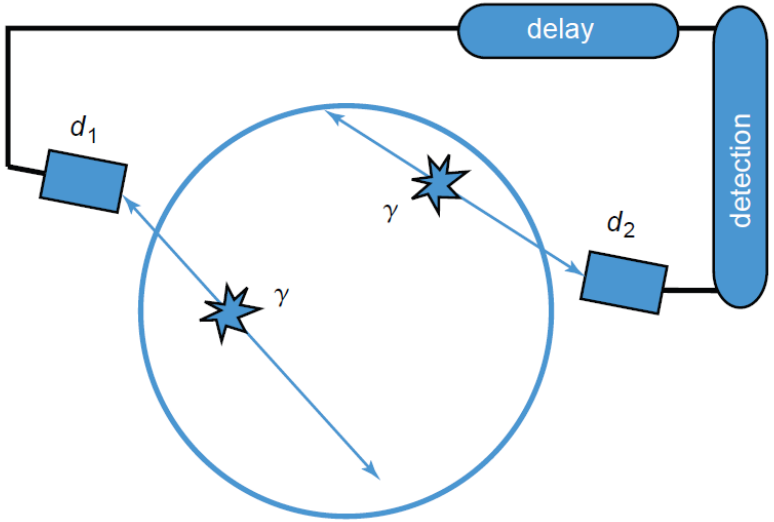

Fig. Schematic representation of a random and its detection. One of the two photons is detected with a small time delay...

Correction for scattered coincidence

- Major sources of scattered radiation for PET signals
  - Scatter within the body.
  - Scatter in the BGO crystal due to poor intrinsic energy resolution
- ~10-15% for 2D PET, and up to 50% for 3D PET
- Correction methods
  - Measure the signal intensity in areas that are outside patient and fit to a Gaussian shape to estimate scatter inside the patient
  - Multiple energy window method
  - Iterative reconstruction based on simulating the actual scatter using CT-derived attenuation maps

Image characteristics

- **Signal-to-noise ratio**
  - **Similar influence factors as SPECT**: radiotracer dose, targeting efficiency, imaging acquisition time, γ-rays attenuation in the patient, system sensitivity, image post-processing, etc
  - **Higher SNR than SPECT due to higher sensitivity**: in the same condition of γ-ray radioactivity, 0.01-0.03% for SPECT, 0.2-0.5% for PET 2D mode, 2-10% for PET 3D mode.
- **Contrast-to-noise:** in addition to SNR, influenced by
  - The correction for in Compton-scattered γ-rays
  - The non-specific uptake of radiotracer in healthy tissue surrounding the pathology being studied.

Image characteristics

➢ Spatial resolution

- The in-plane resolution is much more constant throughout the patient: the inherent "double detection" of two γ-rays reduce the depth dependence of the PSF
- Other factors affecting resolution
  - ✓ The effective positron range in tissue before it annihilates with an electron: 0.2-2.6mm for different radiotracer;
  - ✓ The non-colinearity of the two γ-rays, i.e. the small random deviation from 180°: with FWHM of approximately 0.5°
  - ✓ The dimensions of the detector crystals: an approximate spatial resolution given by half the detector diameter.
- Overall resolution of the system: $R_{\mathrm{sys}} \approx \sqrt{R^2_{\mathrm{detector}} + R^2_{\mathrm{range}} + R^2_{180^{\mathrm{o}}}}$
- Typical FWHM of system resolution: 3-4mm for a small ring system for brain studies, 5-6mm for a larger whole-body system

PET/CT

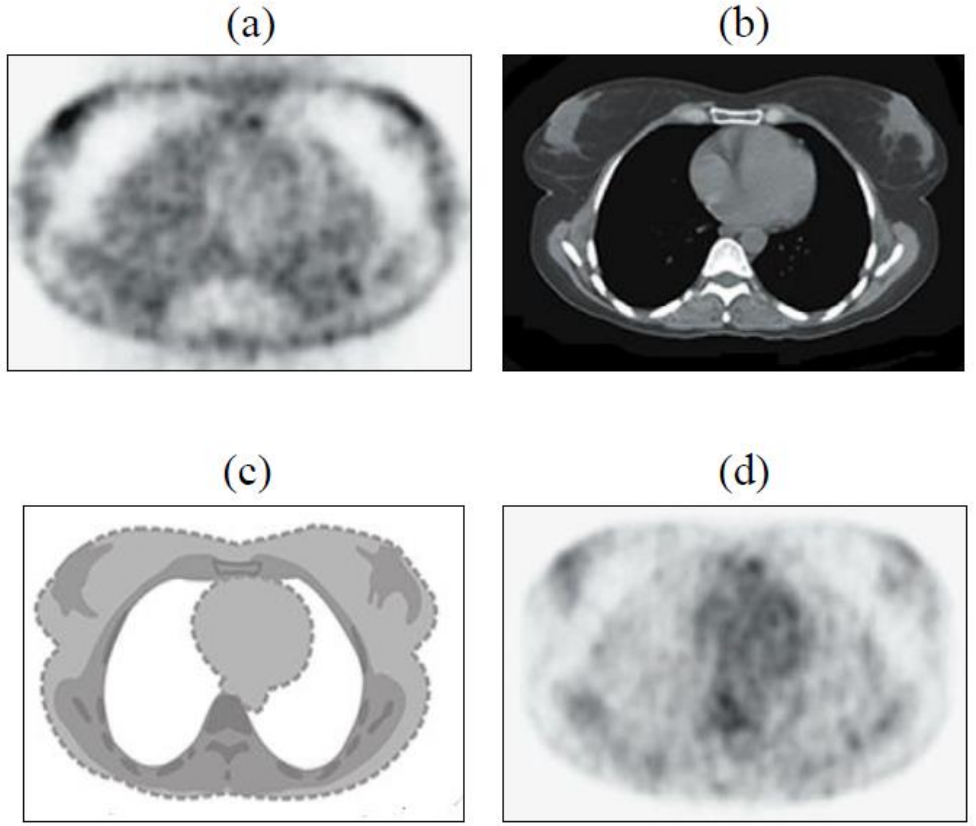

Fig. (left) A PET/CT scanner with two separate rings of detectors. A common bed slides the patient through the two scanners. (right) (a) An uncorrected PET, (b) a CT image, (c) the CT-derived attenuation map after segmentation of the CT image, and (d) the attenuation-corrected PET scan.

Time-of-flight PET

Time-of-flight (TOF, 飞行时间) PET

- Estimating position on the constrained LOR defined by the time difference corresponding to the delay between the two γ-rays;
- The position resolution: $\Delta x = c\Delta t/2$, where Δt is the timing resolution, c is the speed of light
- Constrained LOR reduces the statistical noise since the noise variance is proportional to the length of LOR.
- The multiplicative reduction factor of noise:

$$f = \frac{D}{\Delta x} = \frac{2D}{c\Delta t}$$

where D is the size of patient

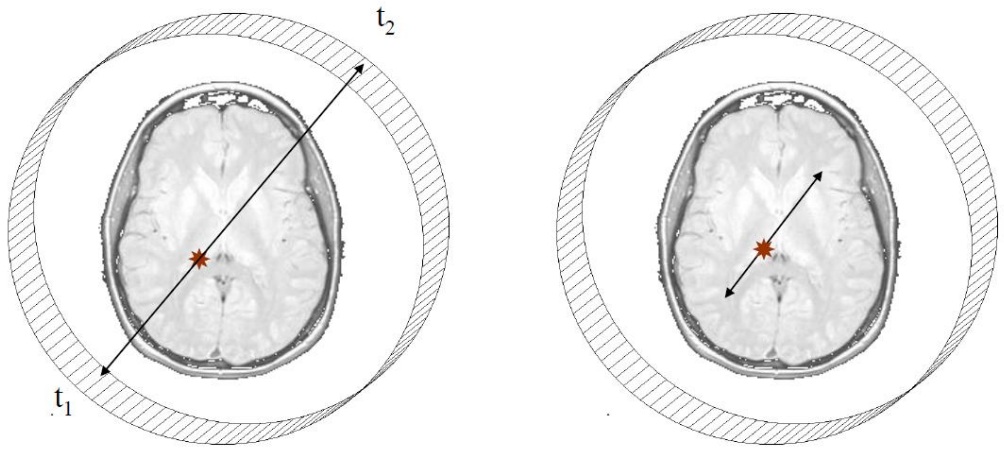

Fig. (left) Conventional LOR formed in PET. (right) Constrained LOR in TOF-PET defined by the time difference t_2-t_1 corresponding to the delay between the two γ-rays striking the particular detectors..

Lecture 10 – PET

This lecture will cover:

– Positron Emission Tomography (PET)

- Introduction of PET
- Radiotracer used for PET/CT
- Instrumentation of PET/CT
- PET imaging
- Data processing in PET/CT
- Image characteristics
- Time-of-flight PET

– Clinical applications of Nuclear Medicine

Bone metabolism

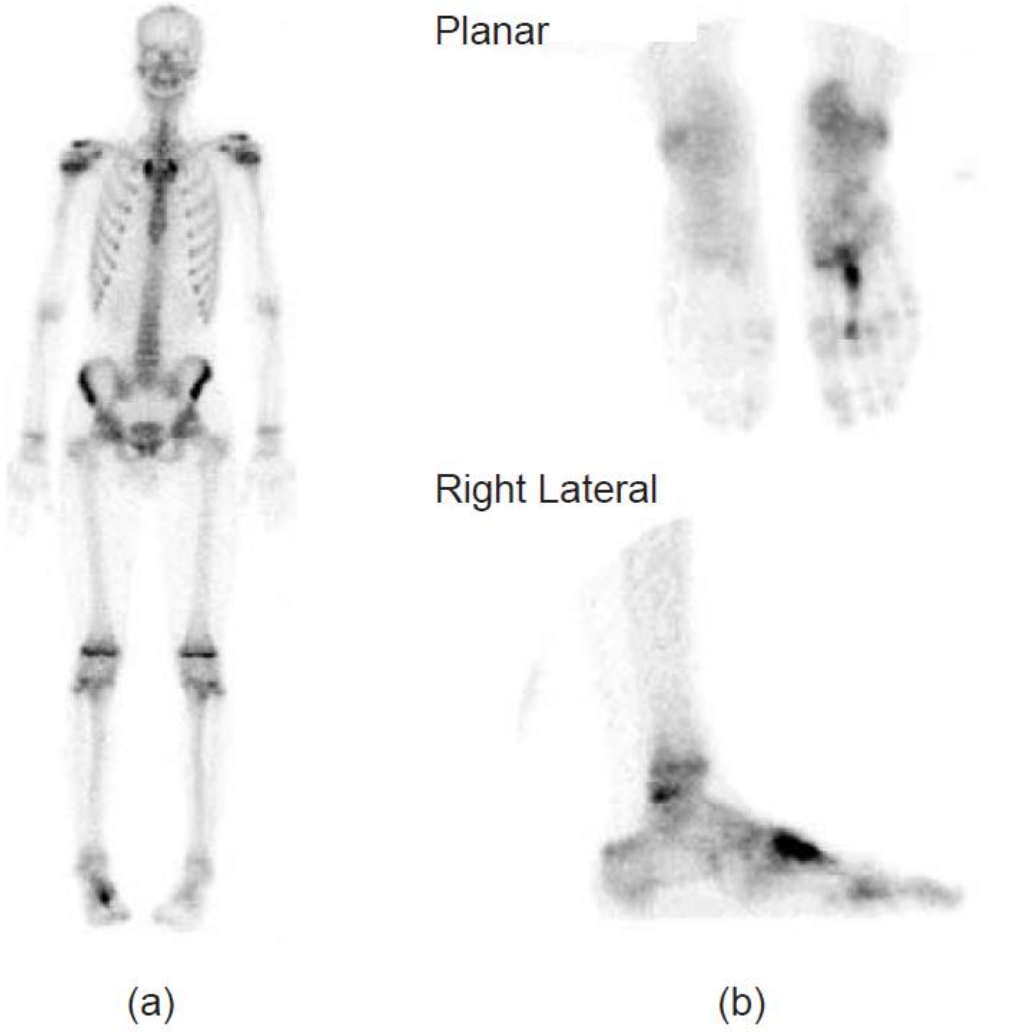

Fig. Left: whole-body scintigraphy after injection of 25 mCi ^{99m}Tc-labeled methylene diphosponate. This patient suffers from a stress fracture of the right foot. Right: control scans show an increased uptake in the metatarsal bone II compatible with a local stress fracture..

Myocardial perfusion

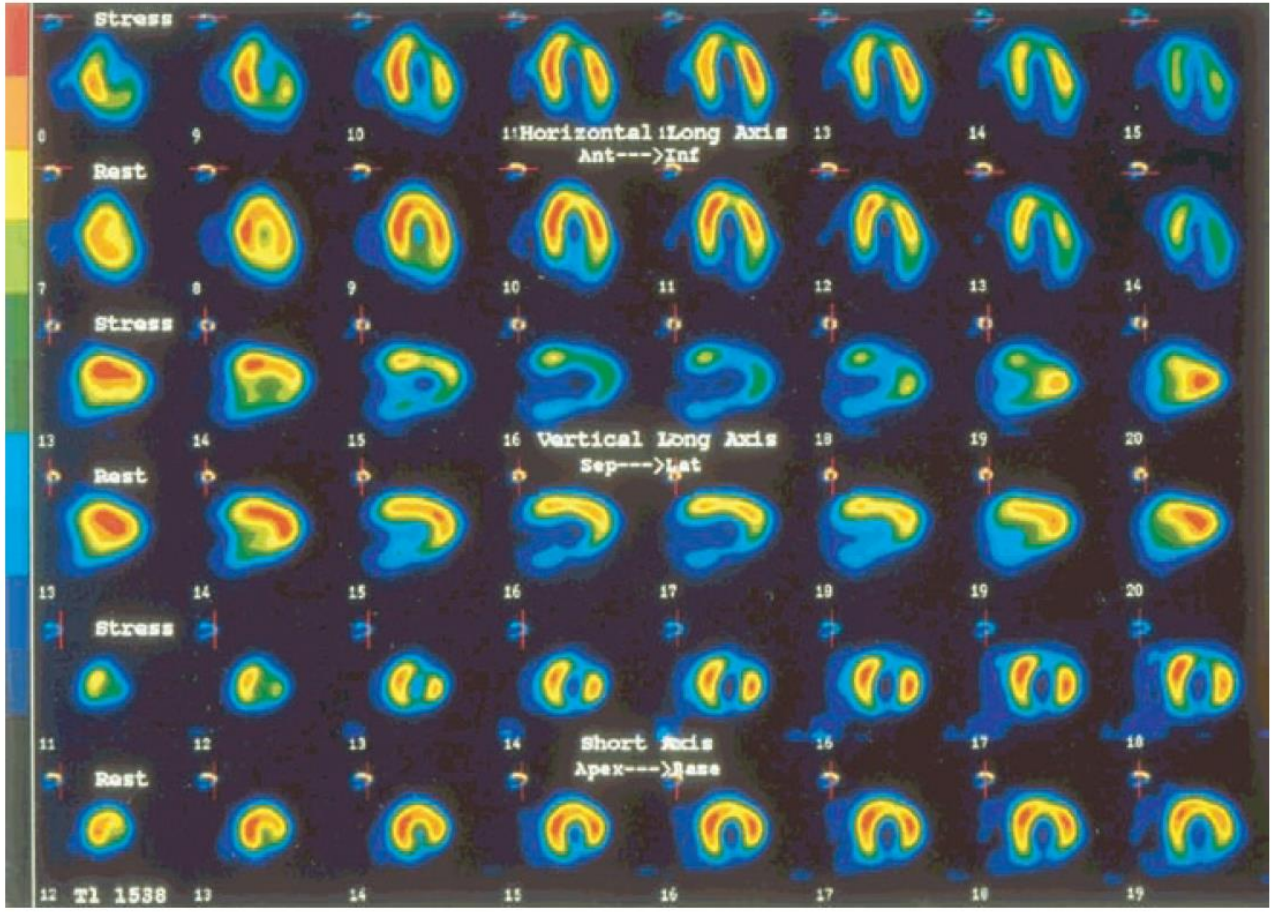

Fig. Myocardial perfusion SPECT scan. Rows 1, 3, and 5 show the myocardial perfusion during a typical stress test. Rows 2, 4, and 6 show the rest images acquired 3 hours later. The first two rows are horizontal long-axis slices, the middle two rows are vertical long-axis slices, and the bottom two rows are short-axis slices. This study shows a typical example of transient hypoperfusion of the anterior wall. On the stress images, there is a clear perfusion defect on the anterior wall (horizontal-axis slice 9, vertical long-axis 16 to 18, short-axis slice 13 to 18). The perfusion normalizes on the corresponding rest images.

Lung embolism

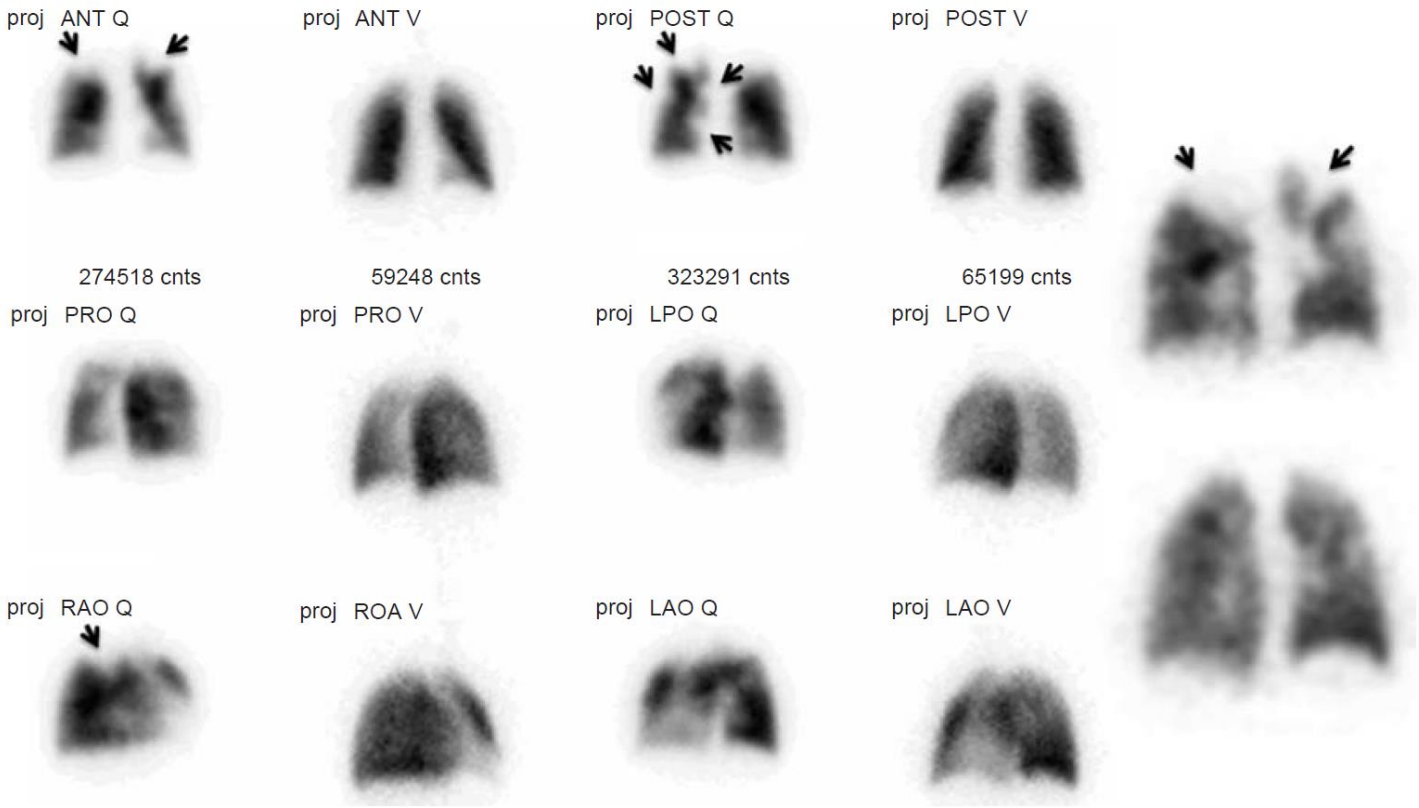

Fig. Lung perfusion (Q) and ventilation (V) scan. The second and fourth columns show six planar projections of a ventilation SPECT scan obtained after the inhalation of radioactive pertechnegas distributed homogeneously throughout both lungs. The first and third columns show the corresponding lung perfusion images obtained after injection of ^{99m}Tc-labeled macroaggregates. Several triangular-shaped defects (arrows) are visible in the perfusion scan with a normal ventilation at the same site. This mismatch between perfusion and ventilation is typical for lung embolism. The fifth column shows a coronal section of the SPECT data set with triangular defects (arrowheads) in the perfusion (upper row) and a normal ventilation (lower row).

Thyroid function

Fig. ^{99m}Tc pertechnetate thyroid scan of a patient with a multinodular goiter. The irregularly enlarged thyroid is delineated. Several zones of normal and increased uptake are visible. Hyperactive zones are seen in the upper and lower pole of the right thyroid lobe. In the right interpolar region there is a zone of relative hypoactivity.

Tumors

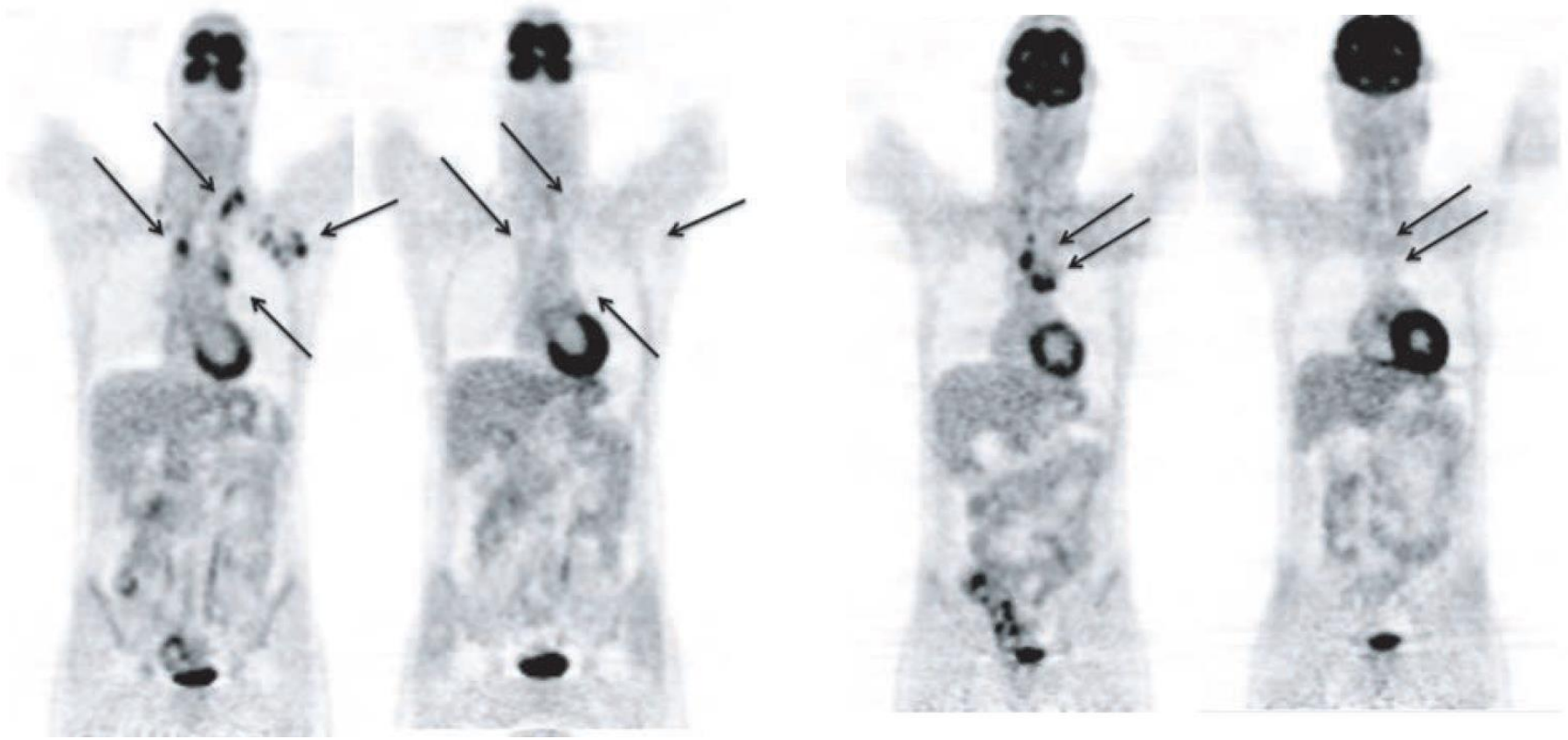

Fig. ^{18}FDG PET scan of a patient suffering from a lymphoma in the mediastinum and the left axilla (1 and 3). The pathological ^{18}FDG uptake in the lymphomatous lymph nodes (arrows) disappeared after chemotherapy (2 and 4)..

Neurological disorders

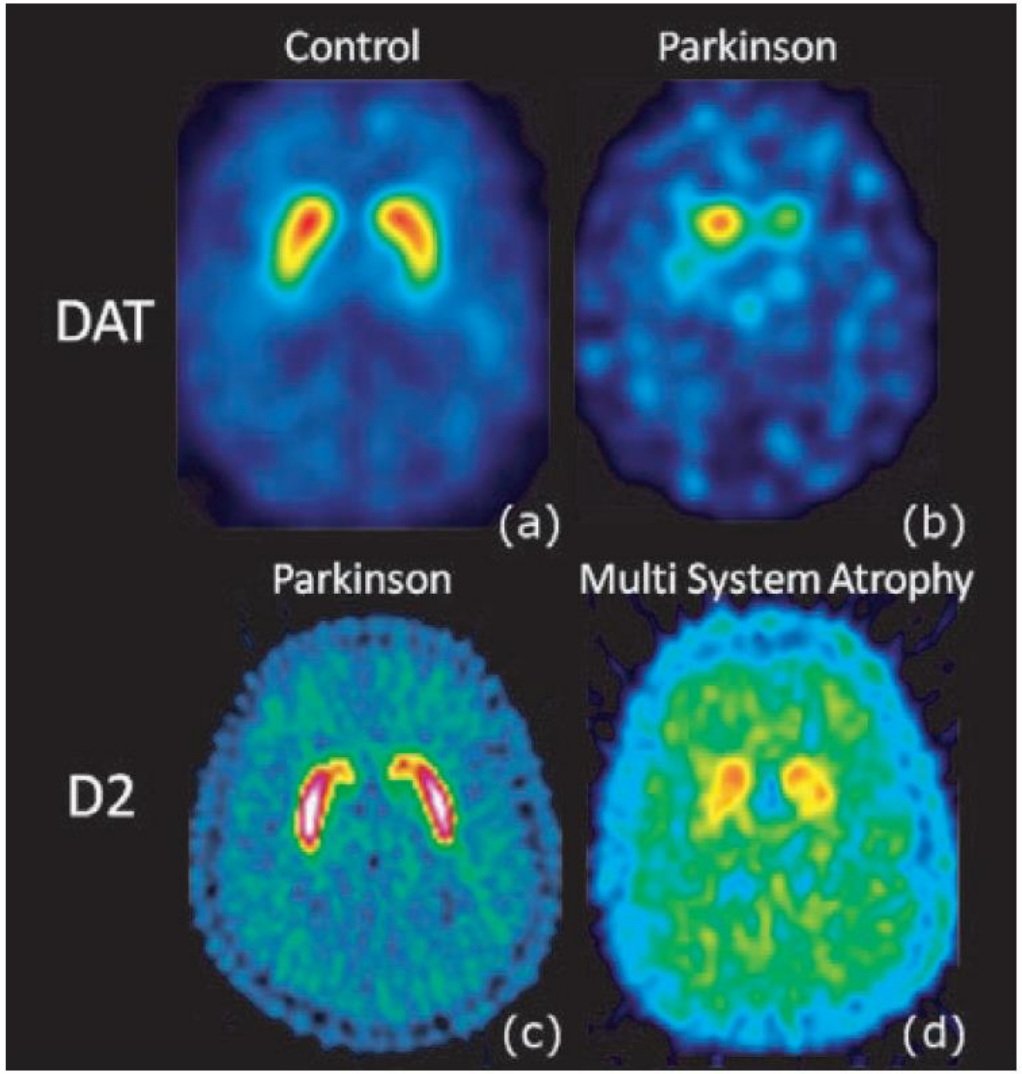

Fig. Upper row: ^{123}I-FP-CIT SPECT scan for presynaptic dopamine transporter (DAT) imaging. Lower row: ^{11}C-raclopride PET scan for postsynaptic dopamine receptor (D2) imaging. (a) Healthy subject. (b,c) In an early Parkinson patient a decrease of the dopamine transporter (DAT) is seen in the basal ganglia while the postsynaptic dopamine receptor (D2) is still normal. (d) Parkinson patient with multi-system atrophia (MSA). The postsynaptic part of the dopaminergic synapse is also impaired.